Volc. Seis., 1996, Vol. 18, pp. 87-106
Reprints available from the publisher
Photocopying permitted by license only

The Use of Multivariate Analysis for Processing Groundwater Precursors of Kamchatkan Earthquakes at the Petropavlovsk Site

A. A. LYUBUSHIN*, G. N. KOPYLOVA**, and Yu. M. KHATKEVICH***

* *Institute of Experimental Geophysics, Joint Institute of Physics of the Earth, Russian Academy of Sciences, Moscow, 123810 Russia*

** *Institute of Volcanology, Far East Division, Russian Academy of Sciences, Petropavlovsk-Kamchatskiy, 683006 Russia*

*** *Seismological Technique Testing Team, Institute of Volcanology, Far East Division, Russian Academy of Sciences, Petropavlovsk-Kamchatskiy, 683006 Russia*

(Received February 23, 1994)

This paper presents the results of a multivariate analysis of changes in groundwater table and chemistry observed in wells and springs at the Petropavlovsk Geodynamic Site during 1986-1992. The objective was to identify time intervals and frequency bands where the scalar time series of the observed parameters showed synchronous behavior. It is supposed that synchronous changes in some or other parameter at different sites or in physically different parameters at one site may be indicative of an imminent earthquake. It is shown that this method help to detect both postseismic synchronous signals and periods of the synchronous behavior of several precursors related to earthquake preparation.

INTRODUCTION

Routine observations at water wells and thermal springs have been conducted at the Petropavlovsk Geodynamic Site, Kamchatka since 1977 in an effort to detect earthquake precursors. These were usually assumed to be those anomalous changes in groundwater parameters which happened to occur before earthquakes. The use of conventional data processing methods (plotting, fitting statistical models of parameter behavior, etc.) and comparisons to seismicity changes have revealed anomalous changes at a number of sites both before and after large earthquakes [7], [9], [10].

This paper presents a follow-up study that continued a search for an optimal groundwater data processing algorithm. It describes the results of a multivariate analysis of data obtained during the 1986-1992 groundwater monitoring. This method for processing different data sets was proposed by one of the authors [13], [14].

The analysis rests on the construction of time-frequency diagrams showing the evolution of the greatest eigenvalue of spectral matrices of multivariate time series with a view to detecting time intervals and frequency bands where the scalar time series representing variations in groundwater table and chemistry, measured in water wells and springs, show a synchronous behavior. It is supposed that synchronous changes in some or other parameter observed at different sites or in physically different parameters measured at one site may be precursory to an earthquake.

This method of analysis used is essentially a statistical technique aimed to reduce data dimensionality and identify the most general informative factors in a set of multivariate and heterogeneous observations. In a historical perspective, the earliest method of this type was the method of principal components which was first intended to analyze covariance matrices in econometrics, psychology, and biology. Further developments along these lines gave birth to the modern method of factor analysis having very diverse applications, including those in geosciences [1]. Examples of similar techniques are the method of identifying significant features in pattern recognition based on the Karhunen-Loeve expansion [17] and the method of orthogonal empirical functions widely used in meteorology [17] and geomorphology [19]. Brillinger [3] extended the method of principal components to the spectral analysis of multivariate time series and applied it to analyze mean monthly temperatures observed at 14 weather stations [3]. A similar approach consists in designing spectral estimators of high frequency resolution using eigenvalues and eigenvectors of a covariance matrix (V. F. Pisarenko's techniques, MUSIC, and EV) [16].

OBSERVATION NETWORK AND DATA SET

The groundwater monitoring stations of the Petropavlovsk Site are situated in the central part of the eastern coast of Kamchatka around the cities of Petropavlovsk-Kamchatskiy and Elizovo (Fig. 1). A detailed description of the geology and hydrogeology of the area can be found in [10].

The Pinachevo station includes a gas-rich flowing GK1 well 1261 m deep and three capped warm springs. The GK1 well discharges pressure thermal water flowing from Cretaceous, Neogene and Quaternary volcanogenic-sedimentary deposits. The Pinachevo station is located in the zone of the northwest-striking Petropavlovsk deep-seated fault which separates the East Kamchatka Volcanic Belt from the nonvolcanic areas of the Malka-Petropavlovsk transverse fault zone [4].

The Pinachevo water has a nitrogen-methane composition, temperature of 5.5°C (spring 3) to 18°C (GK1 well), and mineral content of 0.2 g/l (spring 3) to 9 g/l (GK1 well). The chemical composition varies with the extent of mixing between the fresh groundwater and the rising mineralized chloride calcium-sodium water (the chemical type is defined according to the concentration of components above 25% equiv. units in the order of lower to higher content). For instance, the least diluted water in well GK1 has a chloride calcium-sodium composition, while the composition of much more diluted spring water varies from chloride hydrocarbonate magnesium-sodium (spring 3) to

Figure 1 Location map: *1* - observation site, *2* - earthquake epicenter (I - October 6, 1987, II - March 2, 1992), *3* - volcanoes.

hydrocarbonate chloride sodium (spring 2). The gas emanating from well GK1 is dominated by CH_4 (~80 vol. %) and N_2 (~20 vol. %) and contains Ar (0.12 vol. %), CO_2 (0.23 vol. %), and He (0.23 vol. %). The Pinachevo water is peculiar for its low seasonal flow-rate variation in springs and no seasonal variations at all in the flow rate at GK1 well and in water and gas composition.

The Moroznaya station includes a flowing well (Moroznaya-1), depth 600 m, which discharges pressure water from the Miocene tuff at a flow rate of 1.5 l/s and temperature 15-17°C. The flowing water is sulfate sodium-calcium and has a salt content of 0.2 g/l.

The Moroznaya-1 well shows seasonal changes in water flow rate and temperature, the chemical composition being relatively stable.

The monitoring of springs and wells is done once every three days using a conventional procedure. The water flow is measured with a volume meter, water temperature is measured at the wellhead with a thermometer having a scale division of 0.2°C, and water and gas samples are collected. The water samples are analyzed in the laboratory for a wide range of parameters, including the concentrations of Cl^-, HCO_3^-, H_4SiO_4. The concentration of Cl^- is found by a volumetric argentometer method using thyocyanite and that of HCO_3^- by acidimetry, the end point of titration being recorded by a pH-meter. The concentrations of Cl^- and HCO_3^- are accurate to within 2%. H_4SiO_4 is analyzed using single-beam measurements by a Spekol photoelectric spectrometer with an uncertainty of 10%. Gas samples were analyzed to determine CH_4, N_2, CO_2, Ar, and He using an LKhM-8 gas chromatograph to within ±5%. Air pressure and temperature are

recorded at each station.

The following parameters of wells and springs were chosen for a multivariate analysis: water flow rate and temperature, reliable concentrations of chemical components in water (Cl^-, HCO_3^-, H_4SiO_4), and the chemical composition of free gas at the GK1 well.

The main results obtained at the Pinachevo and Moroznaya stations until 1992 inclusive were presented in [5–10], [18], where discussion was focused on the individual behavior of some water sources and parameters in relation to large earthquakes and to the seismicity of Kamchatka as a whole.

Table 1 Basic information on the 1986-1992 earthquakes that caused changes in the behavior of springs and wells monitored at the Petropavlovsk Site (after [8] and reports of a Seismological Team filed at the Institute of Volcanology, Petropavlovsk-Kamchatskiy).

Earthquake number	*Date*	*Distance from Pinachevo site, km*	*Magnitude*	*Coordinates, deg.*		*Depth, km*
				N lat	*E long*	
1	17.06.1886	160	5.0	53.78	160.66	40
2	06.10.1987	130	6.6	52.85	160.24	34
3	15.09.1989	105	4.9	53.19	160.01	44
4	01.03.1990	120	5.8	53.29	160.23	24
5	19.12.1990	155	6.1	52.77	160.65	24
6	08.04.1991	170	4.7	52.36	158.21	139
7	02.03.1992	115	7.1	52.82	159.99	40

A seismicity increase was observed in the Petropavlovsk Site area in 1986-1992. According to observations at the Petropavlovsk seismograph station, more than sixty earthquakes occurred during that period; they producing shaking of intensities II to VI in and around the Petropavlovsk-Kamchatskiy City. Seven largest earthquakes that occurred close to the stations caused appreciable changes in water behavior (Table 1) [10]. Two M 7.3 and 7.1 earthquakes of intensity VI occurred in the south of East Kamchatka at hypocentral distances of 120-230 km from the stations.

Figure 2 shows some data for 1986-1992. One notes annual seasonal variations for water temperature in springs and for the discharge of Moroznaya well (Fig. 2, *b* and *c*). Variations at GK1 show a unidirectional trend (Fig. 2, *d*). Postseismic changes can be seen in the spring behavior (Fig. 2 *a, c, e,* and *g*) and in the GK1 gas composition (Fig. 2, *h*). The abnormal variations before the October 6, 1987, and March 2, 1992, earthquakes were observed in the concentration of Cl^- for GK1 water (Fig. 2, *d*) and of HCO_3^- for the water at Moroznaya well (Fig. 2, *f*).

The earthquakes (Table 1) were followed by an increase in spring 1 discharge of at least 0.1 l/s (Fig. 2, *a*). It has been shown [5] that postseismic discharge variations are higher at spring 1 than elsewhere, which indicates its higher sensitivity to seismicity. The spring 1 water showed changes in chemical composition after six earthquakes (earthquakes

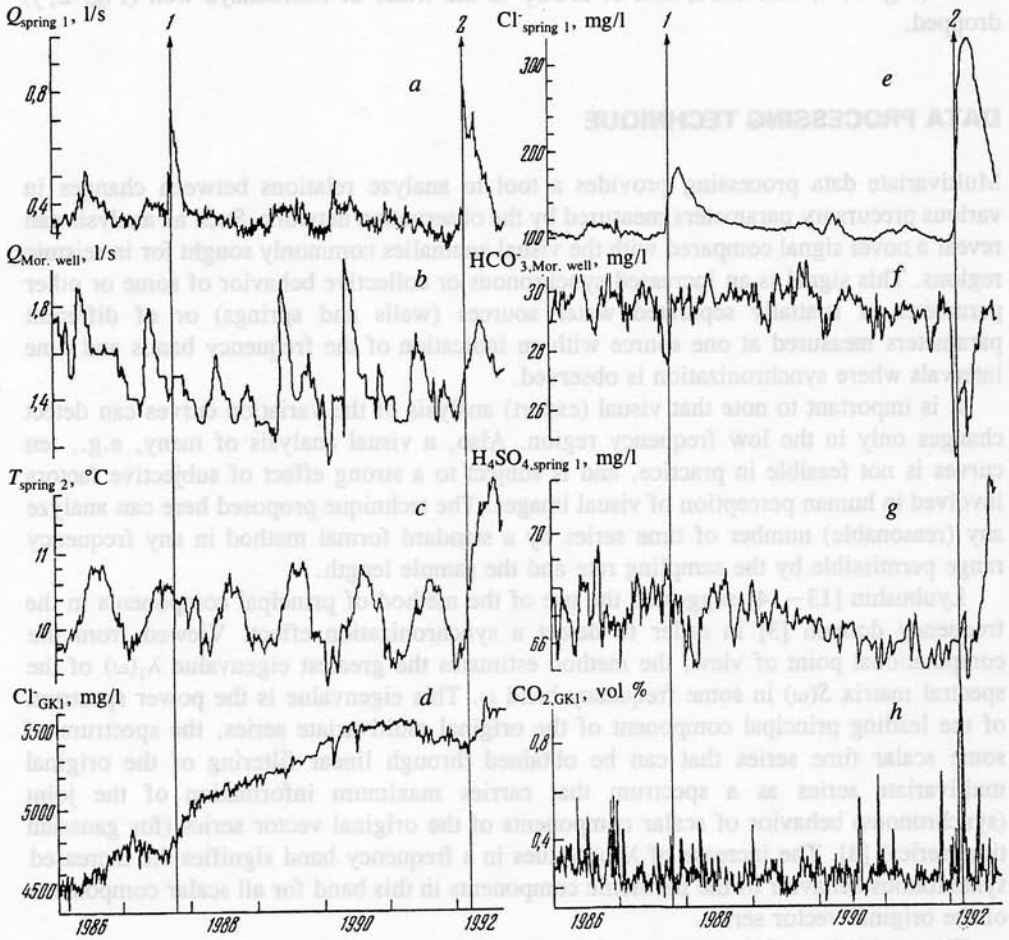

Figure 2 Plots of some source data: *a* — flow rate, spring 1, *b* — flow rate, Moroznaya well, *c* — temperature, spring 2, *d* — concentration of Cl^- in the water of well GK1, *e* — concentration of Cl^- in the water of spring 1, *f* — concentration of HCO_3 in the water of Moroznaya well, *g* — concentration of H_4SiO_4 in the water of spring 1, *h* — concentration of CO_2 in the free gas of well GK1. Vertical arrows mark the times of the earthquakes of October 6, 1987 (1) and March 2, 1992 (2).

1-4, 6, and 7 in Table 1); concentration of Cl^- (Fig. 2, *e*) and some other components increased. Springs 2 and 3 showed a postseismic response to three earthquakes only (2, 4, and 7). Earthquakes 2 and 7 affected the behavior of GK1 and Moroznaya wells. Their epicenters are shown in Fig. 1. Abnormal variations of some parameters were recorded before these earthquakes (magnitude 6.6 and 7.1): the concentration of Cl^- in the GK1

water (Fig. 2, *d*) increased, that of HCO_3^- in the water of Moroznaya well (Fig. 2, *f*) dropped.

DATA PROCESSING TECHNIQUE

Multivariate data processing provides a tool to analyze relations between changes in various precursory parameters measured by the observation network. Such an analysis can reveal a novel signal compared with the visual anomalies commonly sought for in seismic regions. This signal is an increased synchronous or collective behavior of some or other parameter at spatially separated water sources (wells and springs) or of different parameters measured at one source with an indication of the frequency bands and time intervals where synchronization is observed.

It is important to note that visual (expert) analysis of the variation curves can detect changes only in the low frequency region. Also, a visual analysis of many, e.g., ten curves is not feasible in practice, and is subject to a strong effect of subjective factors involved in human perception of visual images. The technique proposed here can analyze any (reasonable) number of time series by a standard formal method in any frequency range permissible by the sampling rate and the sample length.

Lyubushin [13–14] suggested the use of the method of principal components in the frequency domain [3] in order to detect a synchronization effect. Viewed from the computational point of view, the method estimates the greatest eigenvalue $\lambda_1(\omega)$ of the spectral matrix $S(\omega)$ in some frequency band ω. This eigenvalue is the power spectrum of the leading principal component of the original multivariate series, the spectrum of some scalar time series that can be obtained through linear filtering of the original multivariate series as a spectrum that carries maximum information of the joint (synchronous) behavior of scalar components of the original vector series (for gaussian time series) [3]. The increase of $\lambda(\omega)$ values in a frequency band signifies the increased synchronous behavior of the harmonic components in this band for all scalar components of the original vector series.

The evaluation of the greatest eigenvalue $\lambda_1(\omega)$ of $S(\omega)$ in a moving time window having a fixed number of values L, rather than for the entire date sample, gives a two-parameter function $\lambda_1(\tau, \omega)$, where τ is the time coordinate of the window, e.g., the time of its right end. The function $\lambda_1(\tau, \omega)$ can be represented by contour lines or 3D surfaces, where the λ_1 spikes indicate those time intervals τ and frequency bands where the behavior of the scalar components of the original multivariate time series is highly synchronous.

A special feature of geophysical monitoring systems is the physical heterogeneity of the time series recorded at the same or different observation sites. An example is the hydrogeological data from the Petropavlovsk Site. Although the data are heterogeneous, are measured on different scales, and have different amplitudes, the common thing is that all of them are measured at the same time and that they reflect processes that occur in the crust or each reflects some aspect of these processes. Therefore detection of the collective behavior of various hydrophysical and geochemical parameters with indication of the

frequency bands and time intervals where such behavior occurs is of interest for a great variety of monitoring problems. An important constraint, however, is the elimination of the effect of different scales of the scalar components of the original vector time series. Also, because the estimation of the spectral matrix $S(\omega)$ is made in a moving time window for relatively short samples, one should use series in increments before estimating $S(\omega)$ in order to get rid of dominating low frequencies, and then each scalar component should be normalized to have unit sample variance to remove the effect of differing scales. These preliminary operations accomplish a sort of normalization of the spectral matrix in each time window and make it possible to process physically heterogeneous data.

An increase of $\lambda_1(\tau, \omega)$ indicating synchronous changes in different components of a vector series can be caused by the following factors.

1. An external noise source having a long spatial correlation distance and affecting all parameters recorded at the observation sites; this is usually a weather factor (F) producing signal F1.

2. A unidirectional geodynamic process in the crust, in particular, the consolidation of crustal material in the region covered by the observation network — signal F2.

3. Postseismic variations of hydrophysical and geochemical parameters following large earthquakes (in seismically active areas) — signal F3.

Factor 1 can be eliminated through the multivariate compensation of measurable external noise [13], [15].

Synchronization of signals at different sites of an observation network due to the consolidation of small crustal blocks and increased cohesion between them (Factor 2) is the most interesting signal in geophysical terms. We are inclined to think that consolidation of crustal material in a seismic region can sometimes be regarded as an earthquake precursor, because the precursory region must be a solid, compact rock mass [11−12], where energy accumulates without being released in many minor events. The identification of F2 signals in certain frequency bands where significant spikes of $\lambda_1(\tau, \omega)$ occur (i.e., determination of characteristic frequencies of the medium in study area) and the correlation of the time intervals of these spikes with seismic events seem to be important procedures of low-frequency monitoring in seismic regions, capable of revealing new earthquake precursors.

Postseismic variations of hydrophysical and geochemical parameters are another source of signal synchronization at different sites of an observation network (F3 signal). Note that, in the case of low resolution which manifests itself as broad plateaus, where the measured quantities are constant (unfortunately, this was the case in many of our curves), the F3 signal after large earthquakes may be the only synchronous signal, because high resolution is required to detect F1 and especially F2. Moreover, F3 can be a signal of an impending earthquake: the degree of response to small and moderate past earthquakes may show a pattern indicating a future large earthquake (for instance, a regular increase or decrease of $\lambda_1(\tau, \omega)$ spikes).

Below follows a brief description of the technique we used [14]. Let $X(t) = X_1(t),\ldots, X_m(t))^T$; $t = 1,\ldots, L$ be a sample of the original multivariate time series in a window of length L (let this be the first window for the sake of definiteness); m is the dimension of the column vector $X(t)$; t is discrete time (numbering consecutive samples); T is the

transpose symbol. For brevity we shall sometimes omit the argument τ which specifies the time window.

Let us now pass to series in increments:

$$\mathbf{x}(t) = \mathbf{X}(t+1) - \mathbf{X}(t); \quad t = 1, \ldots, L-1, \tag{1}$$

calculate sample estimates of the mean s_i and variance σ_i in a moving window for each component $x_i(t)$ $(i = 1, \ldots, m)$

$$s_i = \sum_{t=1}^{L-1} x_i(t)/(L-1), \quad \sigma_i^2 = \sum_{t=1}^{L-1} (x_i(t) - s_i)^2/(L-2), \tag{2}$$

and normalize each component to unit variance:

$$x_i(t) := (x_i(t) - s_i)/\sigma_i, \quad i = 1, \ldots m. \tag{3}$$

The next step requires estimating the spectral matrix $S(\omega)$. Experience shows that the nonparametric estimator used in [13] (via Fourier transforms in each window and the frequency averaging of multivariate periodograms) does not have high enough frequency resolution for small L. For this reason we will prefer a parametric estimator based on a multivariate autoregressive model [14], [16]:

$$\mathbf{x}(t) + \sum_{k=1}^{p} A_k \mathbf{x}(t-k) = \mathbf{y}(t), \tag{4}$$

where $p \geq 1$ is autoregression order; A_k $(k = 1, \ldots, p)$ are mxm-matrices of autoregression coefficients; $\mathbf{y}(t)$ is the $m-$dimensional series of residuals which is assumed to be a sequence of independent gaussian vectors with a zero mean and covariance matrix $\mathbf{P}$.

The matrices $\mathbf{P}$ and A_k $(k = 1, \ldots, p)$ were found using a Durbin-Levinson procedure with a preliminary computation of the sample estimates of covariance $mxm-$matrices

$$R(k) = \langle \mathbf{x}(t+k)\, \mathbf{x}^H(t) \rangle, \quad k = 0, 1, \ldots, p,$$

where $\langle \ldots \rangle$ denotes time averaging and H is the index of Hermitian conjugation [16].

When $\mathbf{P}$ and A_k $(k = 1, \ldots, p)$ have been determined, the estimate of the complex-valued spectral matrix $S(\omega)$ is found from

$$S(\omega) = F^{-1}(\omega)\, \mathrm{P} F^{-H}(\omega), \tag{5}$$

where the complex-valued matrices $F(\omega)$ are given by

$$F(\omega) = \mathrm{I} + \sum_{k=1}^{p} A_k \exp(-i\omega k). \tag{6}$$

Here, i is the imaginary unit, $\mathbf{I}$ the identity $mxm-$matrix, ω the frequency.

Because $S(\omega)$ is a positive semidefinite Hermitian matrix, its eigenvalues are real and nonnegative. Denote by

$$0 \leq \lambda_m(\omega) \leq \ldots \leq \lambda_2(\omega) \leq \lambda_1(\omega) \tag{7}$$

the $S(\omega)$ eigenvalues arranged in decreasing order, i.e., λ_1 is the largest and λ_m the eigenvalue.

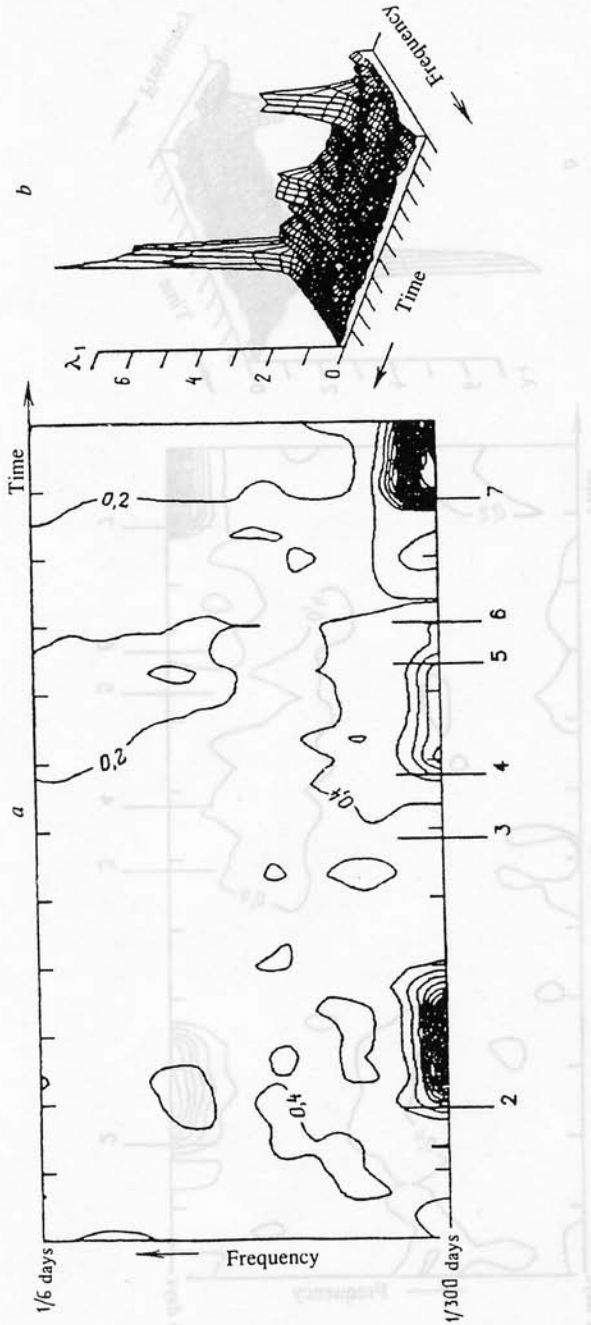

Figure 3 Function $\lambda_1(\tau, \omega)$ for a four-variate series of Cl^- concentrations at Pinachevo site (well GK1; springs 1, 2, and 3). Hereinafter the time marks are given for 6-month intervals. For explanations see the text.

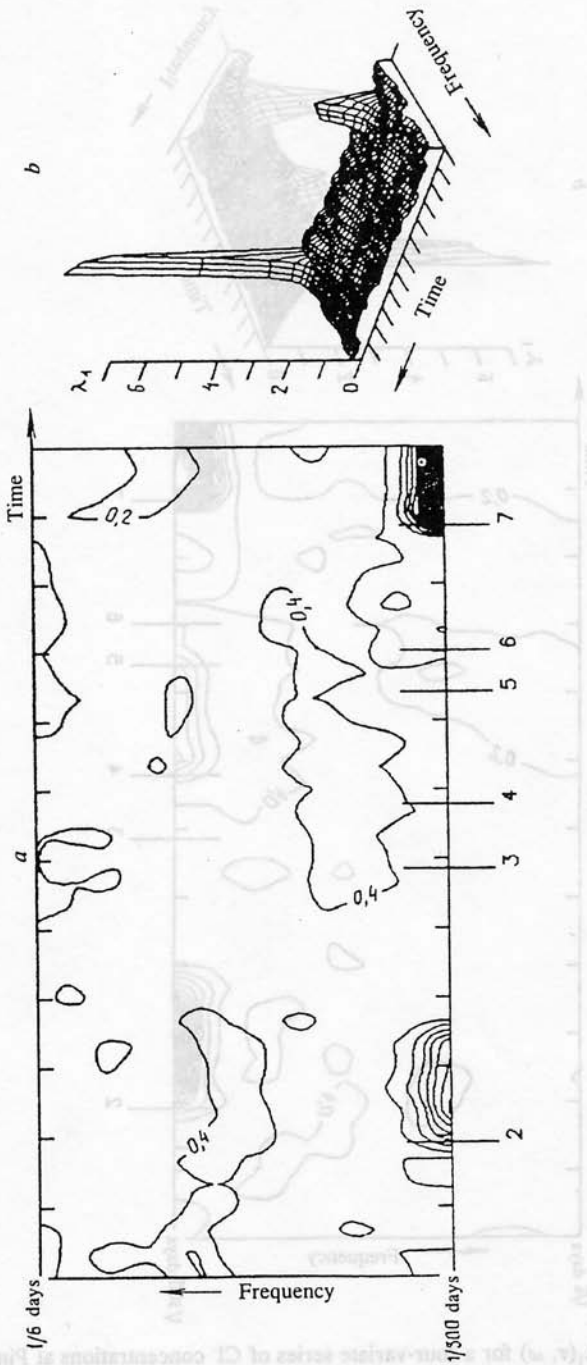

Figure 4 Function $\lambda_1(\tau, \omega)$ for a five-variate series of HCO_3^- concentrations in the water of Moroznaya well and in the Pinachevo water (well GK1; springs 1, 2, and 3).

Further analysis consists in the computation of $\lambda_1(\omega)$ frequency functions in successive time windows of length L shifted at ΔL intervals ($1 \leq \Delta L \leq L$).

RESULTS OF MULTIVARIATE PROCESSING

Figures 3–9 present the $\lambda_1(\tau, \omega)$ functions as contour lines and 3D surfaces for various combinations of the 1986-1992 scalar time series. The contour plots show the times of earthquakes (listed in Table 1) as long numbered vertical lines along the time axis. The spectral matrix was estimated in a moving time window of 100 observations (300 days) shifted at intervals of 20 observations (60 days) using a parametric multivariate autoregression model of third order. The time axis points are the right ends of the moving windows; the time of earthquake 1 is not shown (it is within the first window). The frequency band investigated is determined by the sampling interval, three days (whence the lowest frequency is 1/6 days) and by the window length, 300 days (whence the highest frequency is 1/300 days). The function $\lambda_1(\tau, \omega)$ is presented in the form of contour lines (Figs. 3, a – 9, a), which allows inspection of all details, and in the form of 3D surfaces (Figs. 3, b – 9, b), which allows the fast assessment of the variation scale.

Consider Fig. 3 which shows $\lambda_1(\tau, \omega)$ for four-variate series of Cl^- concentration in water of well GK1 and springs 1, 2, and 3. One can see three significant peaks at low frequencies. Comparison of these peaks with the earthquake times reveals that most of them are F3 signals, i.e., the synchronization was caused by postseismic movements that followed events 2, 4, and 7. It should be noted that the isolines began to grow closer before the peaks were reached somewhat earlier than the events occurred, leading by about 2 weeks for events 2 and 4 and by about 1 month for event 7; that is, the collective behavior of the Cl^- concentrations produced an F2 signal which then graded to F3.

Figure 4 shows $\lambda_1(\tau, \omega)$ for a five-variate series of HCO_3^- concentrations in the water of Moroznaya well and in the springs and GK1 well of the Pinachevo site. It mimics Fig. 3, except for the absence of the intermediate peak, which is a postseismic response to event 4 (that circumstance is of interest on its own account). Note that the concentration of HCO_3^- also shows a passage from precursory synchronization F2 to postseismic F3 for events 2 and 7.

As has been pointed out earlier [10], some of the parameters, the concentrations of Cl^- and HCO_3^- among them, showed anomalous variations recorded 7 months to 27 days before the October 6, 1987, earthquake (event 2), and 9 months to 12 days before the March 2, 1992, earthquake. The multivariate processing [13–14] suggest a new precursor, an intermediate-term (a few weeks to a month) increase of the synchronization of the Cl^- and HCO_3^- concentrations at several springs and wells before these two events, the largest of the earthquakes that occurred in the study area during the last 20 years. They producing shaking of intensity V-VI in Petropavlovsk-Kamchatskiy City.

The function $\lambda_1(\tau, \omega)$ for the four-variate series of H_4SiO_4 concentrations (Fig. 5) shows two significant peaks that look like F3: one (α) occurred after event 4, the other (β) after event 7. Note that the dominant period of the former peak is about three weeks, that of the latter about a month. The plot does not show postseismic synchronization in

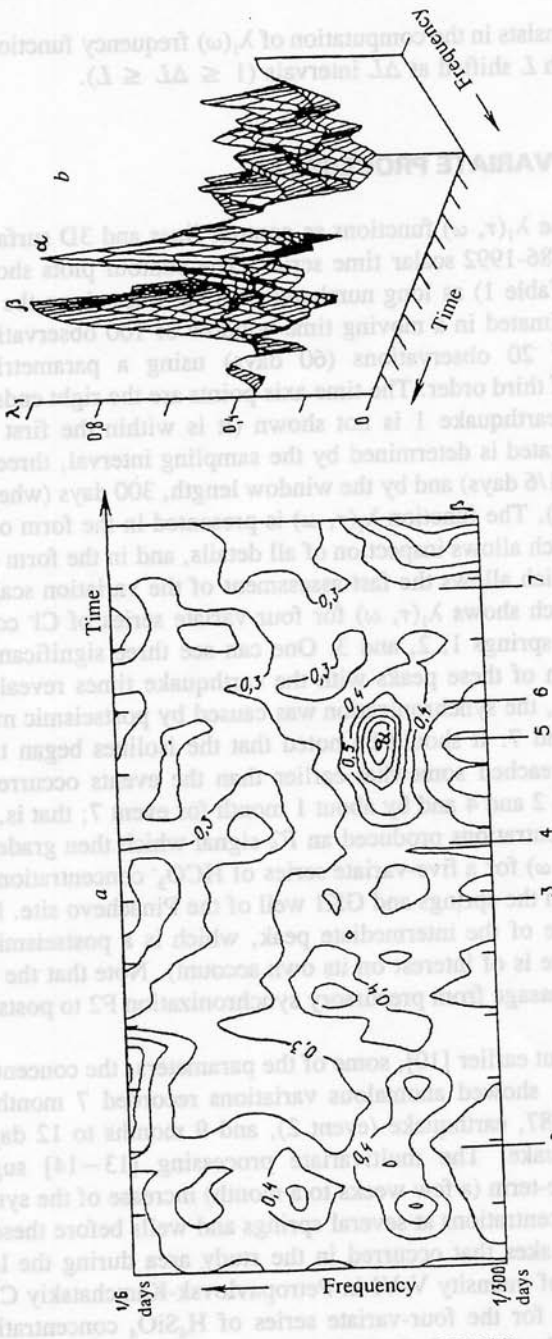

Figure 5 Function $\lambda_1(\tau, \omega)$ for a four-variate series of H_4SiO_4 concentrations in the water of Moroznaya well and Pinachevo site (well GK1; springs 1 and 2); α and β are peaks after events 4 and 7, respectively (see Table 1).

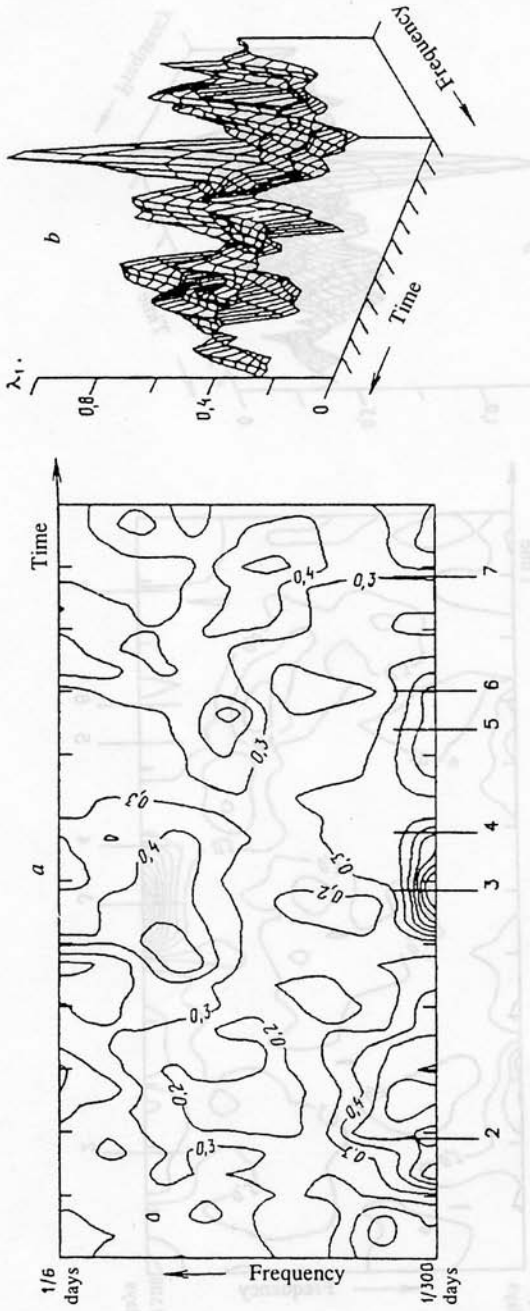

Figure 6 Function $\lambda_1(\tau, \omega)$ for a four-variate flow rate series of the Moroznaya well and Pinachevo site (well GK1; springs 1 and 2).

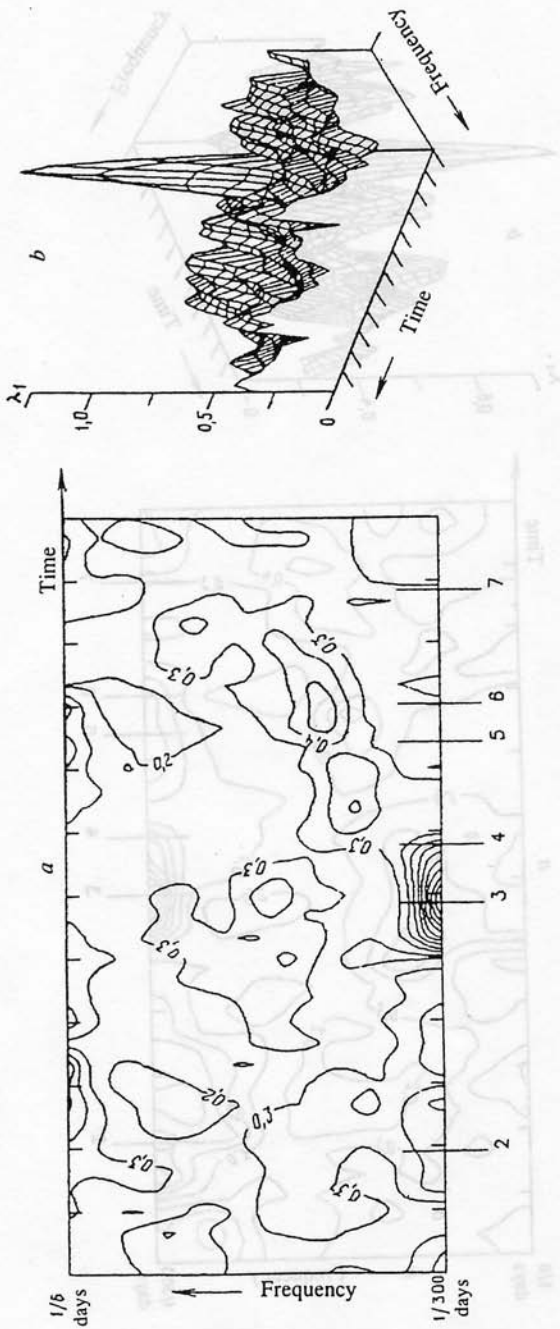

Figure 7 Function $\lambda_1(\tau, \omega)$ for a four-variate series of temperature, flow rate, and the concentrations of HCO_3^- and H_4SiO_4 at Moroznaya well.

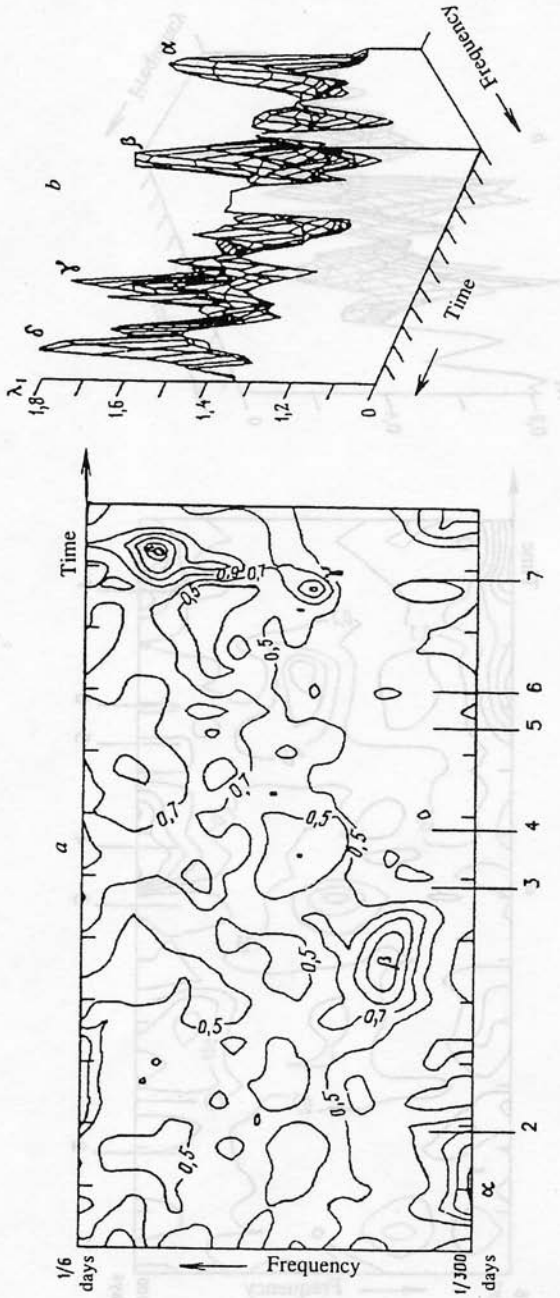

Figure 8 Function $\lambda_1(\tau, \omega)$ for a ten-variate series of flow rate, temperature, and HCO_3^-, Cl^-, H_4SiO_4, Ar, CO_2, CH_4, He, and N_2 concentrations at well GK1; α, β, γ are peaks preceding events 2, 3 and 4, and 7, respectively, δ is a peak after event 7 (see Table 1).

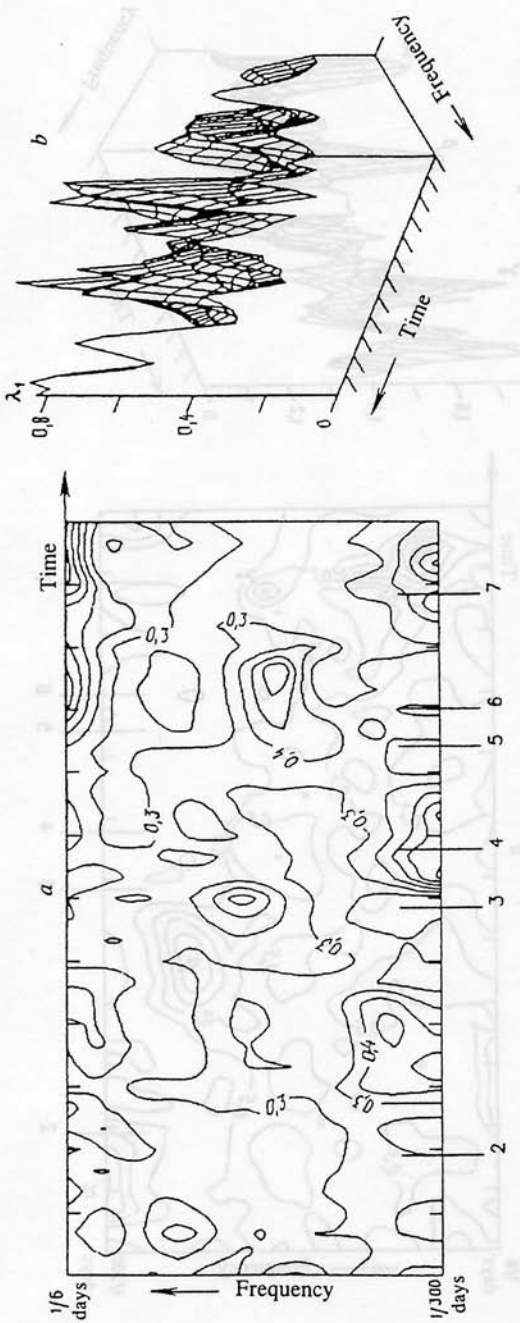

Figure 9 Function $\lambda_1(\tau, \omega)$ for a four-variate series of water temperature at Moroznaya well and Pinachevo well GK1 and springs 1 and 2.

the variation of H_4SiO_4 concentration after earthquake 2 (Table 1). This may indicate essential differences in the geodynamic environment and state of the crust during the preparation and occurrence of earthquakes 2, and also of events 4 and 7, which manifested themselves in the increased synchronization of the H_4SiO_4 concentration in 1990-1992.

Figures 6 and 7 show a synchronous signal at low frequencies in the later half of 1989 and earlier half of 1990. Correlation with the earthquakes (Table 1) suggests that these peaks in the collective flow rate behavior (Fig. 6) and the main parameter values for the Moroznaya well (Fig. 7) can be considered as a precursory and a postseismic synchronization related to events 3 and 4. One notes the absence of a definite response in the collective behavior of the Moroznaya flow rate and other parameters to the preparation and occurrence of the largest earthquakes, 2 and 7. The appearance of synchronous signals in 1989-1990 seems to have been due to a cause other than earthquakes 3 and 4.

Figure 8 summarizes the joint behavior of the main parameters for the GK1 well and shows the most complicated $\lambda_1(\tau, \omega)$ pattern. Four peaks can be seen (λ, β, γ, δ) that stand at moderate heights above the background and have the periods of 300, 25, 14, and 7 days, respectively. It is significant that the peaks migrate with time toward higher frequencies; i.e., synchronization occurs at increasingly shorter variation periods. Correlation with the seismic events suggests that peaks α, β, γ can be classified as F2 signals (precursory synchronization): α before event 2, β apparently preceding events 3 and 4, and γ before event 7. Spike δ seems to be a type F3 postseismic synchronization signal after event 7. Changes in some GK1 parameters (concentrations of Cl^- and free gases) were identified before the October 6, 1987, earthquake (event 2), and especially before the March 2, 1992, earthquake (event 7) [10] (Fig. 2, *d* and *h*). Peak β occurred at about the same time as the peaks in Figs. 6 and 7.

Figure 9 shows a chaotic $\lambda_1(\tau, \omega)$ behavior. This may be a consequence of temperature measurement errors or a too long sampling interval (3 days).

Comparison of Figs. 5–8 shows that the dominant periods for the $\lambda_1(\tau, \omega)$ peaks were 300 to 25 days at all sites for various parameters (flow rate, water chemistry, and free gas composition) during the periods of 1989 and the earlier half of 1991. Those were periods of increased synchronization of the joint behavior of all parameters at all water sources monitored.

The temporal behavior of the observed parameters may have been a consequence of a unidirectional geodynamical process (factor F2) that caused the preparation and occurrence of large earthquakes. Considering that three intensity VI, magnitude $M \geq 7$ earthquakes occurred in the Petropavlovsk Site area in 1992-1993, increased synchronization of the behavior of hydrogeologic parameters at spatially separated wells and springs can be regarded as an intermediate-term precursor of $M \geq 7.0$ earthquakes.

In this analysis we used data that were available for the Pinachevo site since 1979 [9]. The results are not reported here because of a very "quiet" $\lambda_1(\tau, \omega)$ behavior until 1986. In 1986 synchronization began to increase, which is very well seen in Figs. 3–5. The results of the multivariate processing of data at the Petropavlovsk Site revealed two possible varieties of the synchronizing factor F2: a regional geodynamic process (trend

of increasing synchronization) and the process related to the preparation of larger earthquakes.

CONCLUSION

The multivariate analysis of flow rate, water chemistry, and gas composition in wells and springs at the Petropavlovsk Geodynamic Site proved this approach to be promising for converting the art of searching for earthquake precursors into a formal algorithm. This method allows an automatical analysis of an entire frequency band given by the sampling rate and time window length.

The resolution of the procedure based on the estimation of cross-spectral characteristics of observed time series is sensitive to measurement errors and too large sampling intervals. These drawbacks, revealed at the Petropavlovsk Site, rule out the possibility of analyzing high-frequency regions where precursors that are not accessible to visual detection may be concealed. In this context, the Petropavlovsk Site monitoring stations need be equipped with more sensitive pickups and automatic self-contained recording systems that will allow one to use sampling intervals at least as short as one hour.

This method is still far from being perfect. In particular, it is not clear how to discard time series that contain little or no information and just add extra noise. One way to do this is to exclude data series (with a subsequent return) iteratively one by one from the processing and to assess the result of the exclusion through correlation with seismic events. In this way the worst series can be found. The next step will yield the next worst series, and so on, until the good ones remain. This procedure however is time-consuming and inconvenient when many series are to be processed. Also, the formulation of the decision rule (i.e., when an "alarm" is to be declared) remains obscure. In this context our method should be viewed as a data representation technique based on very general statistical ideas for dimension reduction and the identification of the most informative characteristics, and as a program of a search for new precursors, the practical use of which requires good time series (ones with high enough sensitivity and high sampling rate). The resulting $\lambda_1(\tau, \omega)$−diagrams can be useful also for the expert approach, common in practical earthquake prediction when pattern recognition (see patterns in Figs. 3−9) aid in formulating the conclusion about an imminent earthquake based on analogy with precedents.

This work was supported by the Russian Basic Research Foundation, project 94-05-16120.

REFERENCES

1. S. A. Aivazyan, V. M. Bukhshtaber, I. S. Enyukov, and L. D. Meshalkin, *Prikladnaya statistika: klassifikatsiya i snizhenie razmernosti* (Applied statistics: classification and dimension reduction)(Moscow: Finansy i Statistika, 1989).
2. N. A. Bagrov, K. V. Kondratovich, D. A. Ped, and A. I. Ugryumov, *Dolgosrochnye meteorologicheskie prognozy* (Long-term weather forecasting)(Leningrad: Gidrometeoizdat,

1985).
3. D. R. Brillinger, *Time Series. Data Analysis and Theory* (New York: Holt, Rinehart and Winston, 1975).
4. *Geologiya SSSR. T. 31. Kamchatka, Kurilskie i Komandorskie ostrova. Ch. 1. Geologicheskoe opisanie* (Geology of the USSR. Vol. 31. Kamchatka, Kuril and Komandorskie islands. Part 1. Geological description)(Moscow: Nedra, 1964).
5. G. N. Grits, *Volcanology and Seismology* N3 (1986)(cover-to-cover translation).
6. G. N. Grits, *Volcanology and Seismology* N6 (1988)(cover-to-cover translation).
7. G. N. Grits, V. M. Sugrobov, and Yu. M. Khatkevich, *Volcanology and Seismology* N4 (1983)(cover-to-cover translation).
8. V. M. Zobin, E. I. Gordeev, V. F. Bakhtiarov, *et al.*, in: *Zemletryaseniya v SSSR v 1987 g.* (Earthquakes in the USSR in 1987)(Moscow: Nauka, 1990): 116-133.
9. G. N. Kopylova, *Volcanology and Seismology* N2 (1992)(cover-to-cover translation).
10. G. N. Kopylova, V. M. Sugrobov, and Yu. M. Khatkevich, *Volcanology and Seismology* N2 (1994)(cover-to-cover translation).
11. A. A. Lyubushin, Jr., *Izv. AN SSSR. Fizika Zemli* N11: 43-52 (1987).
12. A. A. Lyubushin, Jr., in: *Sovremennye metody interpretatsii seismologicheskikh dannykh* (Modern methods for interpretation of seismological data)(Moscow: Nauka, 1991): 50-61.
13. A. A. Lyubushin, Jr., *Izv. AN SSSR. Fizika Zemli* N3: 103-108 (1993).
14. A. A. Lyubushin, Jr., *Izv. AN SSSR. Fizika Zemli* N7: 135-141 (1994).
15. A. A. Lyubushin, Jr. and L. A. Latynina, *Izv. AN SSSR. Fizika Zemli* N3: 98-102 (1993).
16. S. L. Marple, Jr., *Digital Spectral Analysis with Applications* (Englewood Cliffs, N. J.: Prentice Hall, 1987).
17. K. S. Fu, *Sequential Methods in Pattern Recognition and Machine Learning* (Academic Press, 1968).
18. Yu. M. Khatkevich, *Volcanology and Seismology* N1 (1994)(cover-to-cover translation).
19. S. Christopher, *Geophys. J. Intern.* **116**: 64-84 (1994).